OPEN

PRS GLOBAL OPEN EXPERIMENTAL

Characterization of Inflammatory and Fibrotic Aspects of Tissue Remodeling of Acellular Dermal Matrix in a Nonhuman Primate Model

HaYeun Ji, PhD
Abby Sukarto, PhD
Daniel Deegan, PhD
Frank Fan, BS

Background: Human acellular dermal matrices (hADMs) are applied in various soft tissue reconstructive surgeries as scaffolds to support tissue remodeling and regeneration. To evaluate the clinical efficacy of hADM implants, it is integral that the hADM does not induce a host chronic inflammatory response leading to fibrotic encapsulation of the implant. In this study, we characterized the inflammatory and fibrosis-related tissue remodeling response of 2 commercial hADM products (SimpliDerm and AlloDerm RTU) in a nonhuman primate model using histology and gene expression profiling.

Methods: Eighteen African green monkeys with abdominal wall defects were applied to evaluate the performance of SimpliDerm and AlloDerm RTU implants (N = 3) at 2, 4, and 12-weeks post-implantation. Using histology and gene expression profiling, tissue responses such as implant integration, degradation, cell infiltration, immune response, neovascularization, and pro-fibrotic responses over time were evaluated.

Results: SimpliDerm showed a lower initial inflammatory response and slower implant degradation rate than AlloDerm RTU evidenced by histomorphological analysis. These factors led to a more anti-inflammatory and pro-remodeling microenvironment within SimpliDerm, demonstrated by lower TNFα levels and lower expression levels of pro-fibrotic markers, and promoted tissue repair and regeneration by 3-months post-implantation.

Conclusions: Overall, histology and gene expression profiling analyses shown in this study demonstrated an effective model for analyzing hADM performance in terms of host inflammatory and fibrotic response. Further studies are warranted to fully evaluate the utility of this novel hADM in the clinical setting and verify the prognosis of our pre-clinical analysis model. *(Plast Reconstr Surg Glob Open 2021;9:e3420; doi: 10.1097/GOX.0000000000003420; Published online 16 February 2021.)*

INTRODUCTION

Human acellular dermal matrices (hADMs) are often used in reconstructive surgical applications[1–4] due to their biocompatibility and ability to support tissue regeneration over time.[5,6] Derived from human skin, hADMs are composed primarily of collagen and other extracellular matrix (ECM) proteins, which serve as both a structural scaffold and bioactive modulators for promoting proper tissue remodeling and regeneration.[7] One major concern with using hADMs is the potential occurrence of a chronic host inflammatory response that can lead to implant rejection, fibrotic encapsulation, and/or reoperation.[8] To avoid adverse reaction, hADMs are processed to remove immunogenic cellular components and often terminally sterilized to reduce bioburden.[9,10] However, the usage of chemicals and reagents during these processes may alter the ECM structure, which can negatively influence the regenerative potential of the hADM.[11] The ideal scaffold for host tissue regeneration would be the native ECM in the host tissue; thus, efforts have been made to develop a new type of hADM, SimpliDerm, using exclusive proprietary

From the Aziyo Biologics, Inc., Silver Spring, Md.

Received for publication October 13, 2020; accepted December 10, 2020.

DOI: 10.1097/GOX.0000000000003420

Disclosure: *AS, DD, and FF are current employees of Aziyo Biologics, Inc., manufacturer of SimpliDerm. HJ was an employee of Aziyo Biologics, Inc. during the time of this study.*

Related Digital Media are available in the full-text version of the article on www.PRSGlobalOpen.com.

methodology for processing and sterilizing grafts that best preserve the native ECM architecture.

This study evaluates hADM integration by comparing histology and gene expression in a nonhuman primate (NHP) model. NHPs such as the African green monkey, whose genome has >90% homology to the human genome,[12] have been widely used in pre-clinical studies to predict the immunologic response to hADM implants in humans.[13,14] By using immune-competent animals such as NHPs, it is possible to better evaluate the immunological tolerance of hADMs in a clinically relevant setting to form a predictive model of tissue integration and regeneration post-implantation.[14,15] As the immune system is an active component of tissue remodeling, characterizing the level of associated inflammatory cells, cytokines, and growth factors during hADM integration and tissue regeneration is integral for the evaluation of hADM performance. Although previous NHP studies have performed histomorphological evaluation of hADMs upon implantation[13,14,16,17] and characterized the inflammatory and fibrotic response using histological and cytokine analysis,[13,16] we are not aware of any evaluations performed at a genetic level. Studying the temporal gene expression profile of an implanted hADM allows for a better quantification of cell function over time and earlier prediction of responses that may express phenotypically at a later time point.[18,19]

The objective of the current study was to characterize the inflammatory and fibrosis-related tissue remodeling response to 2 commercial hADMs (SimpliDerm and AlloDerm RTU) in a NHP model using histology and gene expression profiling. We speculated that observing these responses through histology and gene expression would allow for a more accurate prognosis of the hADM performance in a clinical setting.

MATERIALS AND METHODS

hADM Product Information

Commercially available hADMs used were (1) SimpliDerm (Aziyo Biologics, Silver Spring, Md.; 1.3–1.4 mm thickness[9]) and (2) AlloDerm RTU (Allergan, Madison, N.J.), Thick.[10]

NHP Animal Study Design

The experimental procedure was approved and conducted by the Institutional Animal Care and Use Committee of the Behavioral Sciences Foundation, St. Kitts, Eastern Caribbean. Eighteen African green monkeys weighing approximately 3.5–6 kg were included in the study. Animals were randomly assigned so that 9 animals were implanted with SimpliDerm graft pieces and the other 9 with AlloDerm RTU graft pieces, each cut to a size of 3 cm × 7 cm. There were 3 animals for each time point of 2, 4, and 12-weeks per hADM group. Upon implantation surgery, an abdominal wall defect was created by making a longitudinal mid-abdominal incision of approximately 7 cm to expose an area of the linea alba and muscle wall. The incision was expanded bilaterally 1.5 cm in each direction to create a 3 cm × 7 cm full thickness window defect, where appropriate graft piece was implanted. Animals were euthanized and the explant was harvested for post-assessments at 2, 4, and 12-week time points. Further details on the procedure are described in Supplemental Digital Content 2. (**See appendix, Supplemental Digital Content 2,** which displays details of the non-human primate model study. http://links.lww.com/PRSGO/B580.)

Immunohistochemical Staining

Tissue samples were fixed in 10% Neutral Buffered Formalin (StatLab, McKinney, Tex.), paraffin-embedded, sectioned, and stained using the standard hematoxylin and eosin (H&E), Verhoeff-van Gieson (VVG), and Masson's Trichrome (MT) staining procedures. For antibodies, mouse anti-human monoclonal antibodies to Col IV and CD68 (Pre-diluted and ready to use; Biocare Medical, Pacheco, Calif.) and a mouse HRP-Polymer Kit (Pre-diluted and ready to use; Biocare Medical, Pacheco, Calif.) were used. The slides were imaged using an Olympus BX41 microscope and EP view software (Olympus, Shinjuku, Japan).

Histomorphological Evaluation

Histomorphologic analyses were scored in a blinded manner by an independent histopathologist according to a scoring matrix (Table 1), and the data were represented as the group mean and SD. Implant thickness was determined by averaging five random widths along the length of the tissue section using ImageJ analysis software.

Gene Expression Analysis

Real-time, quantitative reverse transcription polymerase chain reaction (qPCR) was conducted to quantitatively measure the gene expression levels of SimpliDerm and AlloDerm RTU explants at each time point. Samples (1 mm × 1 mm) cut from the middle of the implant were minced and homogenized in 300 µL TriReagent (Molecular Research Center, Cincinnati, Ohio) and ribonucleic acid (RNA) was extracted using a Direct-zol RNA MiniPrep Kit (Zymo Research, Irvine, Calif.). Complementary deoxyribonucleic acid (cDNA) was synthesized using a High Capacity cDNA Reverse Transcription Kit (Applied Biosystems, Foster City, Calif.). Gene-specific primers (Table 2) were designed using Primer 3 software.[20] qPCR was performed on a BioRad CFX384 Real Time System (BioRad, Hercules, Calif.). The relative gene expression levels were determined using the ΔΔCT calculation method described by Haimes et al,[21] where gene expression levels at each time point were normalized to the 2-week time point of each group, and GAPDH was used as an endogenous control.

Protein Expression Analysis using ELISA

The amount of tumor necrosis factor TNFα protein in frozen samples was measured using a TNF-alpha DuoSet ELISA kit (R&D Systems, Minneapolis, Minn.) according to manufacturer protocol. For frozen sample preparation, approximately 500 mg were minced and mixed with 2 mL PBS with protease inhibitor cocktail (Sigma, St. Louis, Mo.). Tissues were homogenized using a hand-held homogenizer (Omni International, Kennesaw, Ga.) on

Table 1. Histomorphology Scoring Matrix

Score	Inflammation/Inflammatory Cells
0	Absent
1	Rare, minimal ~1–5 per high power field (hpf; 40x obj)
2	Mild, uncommon multifocal or localized, ~5–10/hpf
3	Notable, regionally extensive or confluent infiltrate, with preservation of local architecture
4	Packed, with effacement of regional architecture
Score	**Neovascularization**
0	Absent
1	Minimal capillary proliferation, focal, 1–3 buds
2	Groups of 4–7 capillaries with supporting fibroblastic structures
3	Broad band of capillaries with supporting structures
4	Extensive band of capillaries with supporting fibroblastic structures
Score	**Fibrosis**
0	Absent
1	Minimal, narrow band, ~1–2 cell layers thick
2	Thin, localized band, ~<10 cell layers thick
3	Moderately thick, contiguous band along length of tissue
4	Extensive, thick zone with effacement of local architecture
Score	**Other Pertinent Microscopic Observations**
0	No response
1	Minimal/focal/barely detectable
2	Mild/focal or rare multifocal/slightly detectable
3	Moderate/multifocal to confluent/easily detectable
4	Marked/diffuse/overwhelming presence

ice. The resulting suspension was centrifuged for 15 min at 1500 × g to collect the lysate.

Statistical Analysis

All tests were conducted in triplicate and presented as the group mean and SD, unless stated otherwise. All variables passed assessment for normality. Statistical significance was analyzed using the student's t test for comparing 2 means, and 1-way ANOVA with Tukey's post-hoc analysis for comparing multiple samples. Statistical significance was set at $P < 0.05$.

RESULTS

Histomorphological Evaluation

At 2-weeks post-implantation, integration did not occur for either hADM product, and thus, histological analysis was not performed. At 4-weeks post-implantation, the H&E staining of SimpliDerm showed definite implant presence, as represented by darker pink regions (Fig. 1A). This was also indicated in MT staining that distinguishes the implant collagen (darker blue) from newly deposited collagen (lighter blue) (Fig. 1B) and in VVG staining that showed the presence of residual implant elastin (black). (**See figure, Supplemental Digital Content 1,** which displays histomorphological evaluation of SimpliDerm and AlloDerm RTU implants at 4 and 12 weeks. VVG and MT images of SimpliDerm (A, C, E) and AlloDerm RTU (B, D, F) implants harvested after 4 and 12 weeks post-implantation. The implant presence is not distinctive for either hADM. A 500 μm scale bar is shown. http://links.lww.com/PRSGO/B579.) H&E staining also indicated moderate levels of cellular infiltration across the implant site and at the implant and host tissue interface. The measured tissue thickness of AlloDerm RTU was 32.29 ± 17.7 % thinner than SimpliDerm ($P = 0.04$; Fig. 1D–E). Immunohistochemistry staining against CD68 (a pan macrophage marker) showed that SimpliDerm implants demonstrated mild inflammation expected during early implant integration (Fig. 1C), whereas AlloDerm RTU showed a greater inflammatory response with highly concentrated areas of robust macrophage and giant cell infiltrates within the center of the implant (Fig. 1F).

At 3-months post-implantation, the implant was not visible in both SimpliDerm and AlloDerm RTU (Fig. 1G–H). VVG images showed that elastin fibers were noted at minimal levels in association with all implant sites (**See figure, Supplemental Digital Content 1,** which displays histomorphological evaluation of SimpliDerm and AlloDerm RTU implants at 4 and 12 weeks. VVG and MT images of SimpliDerm (A, C, E) and AlloDerm RTU (B, D, F) implants harvested after 4 and 12 weeks post-implantation. The implant presence is not distinctive for either hADM. A 500 μm scale bar is shown. http://links.lww.com/PRSGO/B579.). Fibroblast was found to evenly spread throughout the tissue for both groups, indicating greater cell infiltration than previously seen at earlier time points. The lack of acellular regions, presence of fibroblasts, and new collagen deposition all suggested that tissue remodeling was persistent within and surrounding the abdominal wall implant site for both implants tested. The inflammatory response was also mild in both SimpliDerm and AlloDerm RTU groups at this time point (Fig. 1I–J).

For all groups and time points, there was no presence of implant-associated fibrin, necrosis, mineralization, osseous metaplasia, or cavity/pocket formation (e.g., seroma).

Table 2. Sequences of Gene-specific Primers for qPCR Analysis

Gene	Accession #	Description	Primers
Col1a1	XM_008011525.1	Collagen type 1 alpha 1	F: GCGGAAATGATGGTGCTACT R: ACCAGGTTCACCGCTGTTAC
Col3a1	XM_007965602.1	Collagen type III alpha 1	F: GGCATCCCAGGAGAAAAGGGTC R: GCCACCTCGTTCTCCATTCTT
VEGFA	XM_007972427.1	Vascular endothelial growth factor A	F: TAAGTCCTGGAGCGTTCCCT R: ACGCGAGTCTGTGTTTTTGC
COL4A1	XM_007960883.1	Collagen type IV alpha 1	F: TTTTGTGATGCACACCAGCG R: TCATACAGACTTGGCAGCGG
TGFβ1	XM_007996894.1	Transforming growth factor beta 1	F: CAGCATGTGGAGCTGTACCA R: CCGGTAGTGAACCCGTTGAT
αSMA	XM_007963488.1	Actin alpha 2, smooth muscle (ACTA2)	F: AGCCAAGCACTGTCAGGAATC R: CTCTTCAGGGGCAACACGAA
CTGF	XM_008007024.1	Connective tissue growth factor	F: CGGGAAATGCTGTGAGGAGT R: CTTCCAGTCGGTAAGCCGC
LH2b	XM_008008830.1	Lysyl hydroxylase 2 or procollagen-lysine,2-oxoglutarate 5-dioxygenase 2 (PLOD2)	F: ACTCCCCTACTCCGGAAACA R: AGCAGTGGATAACAGCCTTCC
GAPDH	XM_007967342.1	Glyceraldehyde-3-phosphate dehydrogenase	F: GGGAGCCAAAAGGGTCATCA R: CGTGGACTGTGGTCATGAGT

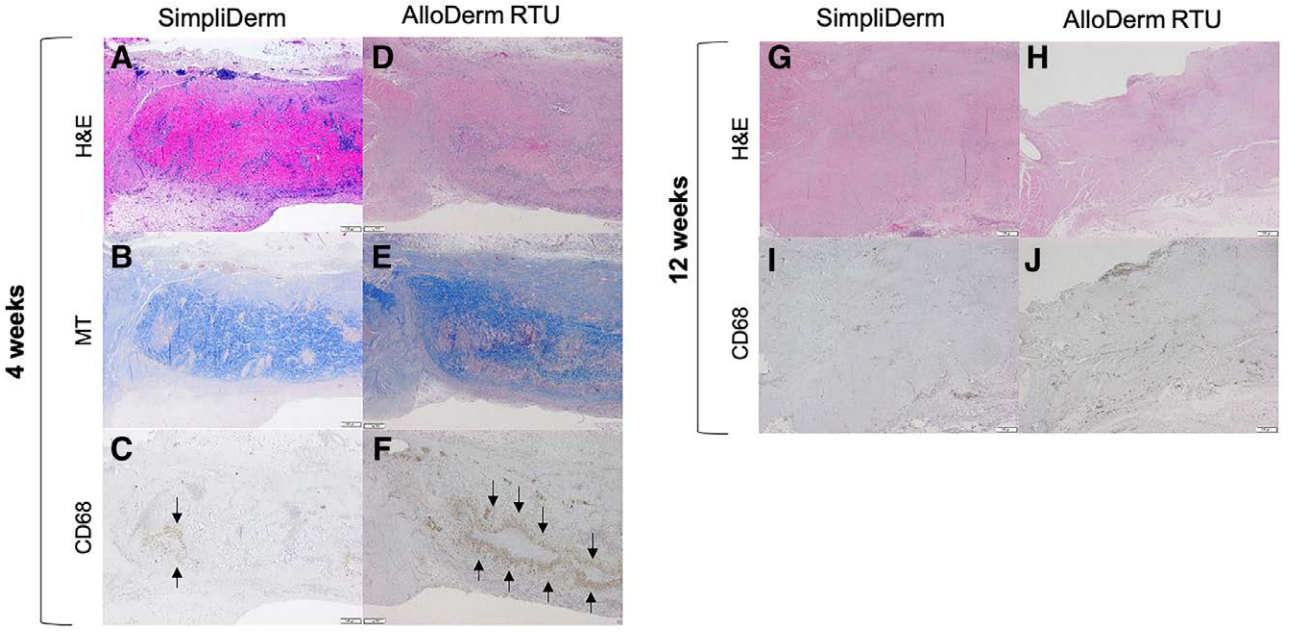

Fig. 1. Histomorphological evaluation of SimpliDerm and AlloDerm RTU implants at 4 and 12 weeks. Histology images of H&E, MT, and immunostaining against CD68 images of SimpliDerm (A–C, G, I) and AlloDerm RTU (D–F, H, J) implants harvested from the abdominal wall of NHP after 4 weeks and 12 weeks post-implantation. Darker contrast regions indicate hADM implants, whereas lighter regions represent host tissue. Arrows shown on CD68 images (C, F) indicate the presence of CD68-positive inflammatory cells. A 500 μm scale bar is shown.

Inflammatory Cell Subtypes

To further elucidate the inflammatory response within the implant, inflammatory cell subtypes were scored (Fig. 2A) and analyzed based on the histomorphology scoring matrix (Table 1). At 4 weeks, neutrophils were present with a score of 2.00 ± 0.50 and macrophages with score of 2.50 ± 0.50 in SimpliDerm. However, for AlloDerm RTU, neutrophils were present at significant lower population than macrophages (1.50 ± 0.00 and 3.17 ± 0.76, respectively; $P = 0.02$). Lymphocyte population score was 2.33 ± 0.29 in SimpliDerm and 1.67 ± 0.58 in AlloDerm RTU. Giant cell population score was 2.67 ± 0.52 in SimpliDerm and 3.00 ± 0.00 in AlloDerm RTU. There were no plasma cells, eosinophils, or foam cells present in either group.

At 3 months, the overall inflammation was decreased in both groups. The overall inflammation score was decreased by 45.05 % for SimpliDerm, from 3.33 ± 0.58 at 4 weeks to 1.83 ± 0.29 at 3 months, and by 47.71 % for AlloDerm RTU, from 3.50 ± 0.50 at 4 weeks to 1.83 ± 0.29 at 3 months. In both groups, macrophages were the most prominent cell type, yet their presence was at mild–moderate levels, whereas giant cells and lymphocytes were present at minimal levels. Neutrophils, eosinophils, and foam cells were absent in both groups.

In addition, the protein expression of pro-inflammatory TNFα at the implant and surrounding host abdominal tissue was measured using ELISA. Although there was no significant difference in the TNFα levels between SimpliDerm and AlloDerm RTU groups at 4 weeks, the TNFα level in the AlloDerm RTU group was significantly higher than that of the SimpliDerm group at 3 months (146.66 ± 41.33 versus 37.51 ± 43.02 pg TNFα /mg protein; $P = 0.034$; Fig. 2B).

Collagen Synthesis and Vascularization

Genes encoding the synthesis of collagen type I and III, *Col1a1* and *Col3a1*, respectively, were evaluated at all time-points to determine the rate of collagen synthesis within both implants. The expression levels of *Col1a1* and *Col3a1* (each normalized to their 2-week time point) increased over time for SimpliDerm and AlloDerm RTU (Fig. 3A-B). For instance, SimpliDerm demonstrated a ~15-fold increase of *Col3a1* at 12 weeks, whereas AlloDerm RTU exhibited a ~43-fold increase at the same time point (Fig. 3A). Similarly, the SimpliDerm expression level of *Col1a1* increased to ~14-fold at 12-weeks post-implantation, whereas that of AlloDerm RTU increased significantly to ~49-fold at 12 weeks (Fig. 3B). Thus, the increase in *Col1a1* and *Col3a1* expression levels from 2 to 12 weeks was significantly higher in AlloDerm RTU than that of SimpliDerm ($P = 0.04$ for *Col1a1* and $P < 0.001$ for *Col3a1*). These results suggest that collagen type I and III expression increased in greater levels within AlloDerm RTU than SimpliDerm over time.

To assess the degree of vascularization within implants, expression levels of 2 major blood vessel-associated genes, vascular endothelial growth factor (*VEGF*) and collagen type IV (*Col4a1*), were evaluated. AlloDerm RTU showed higher increases in *VEGF* and *Col4a1* expression levels by 12-weeks than SimpliDerm (Fig. 3C–D). At 12 weeks, SimpliDerm showed a minimal fold-increase barely over baseline value of *VEGF* expression, whereas AlloDerm RTU demonstrated a significantly higher level of *VEGF* upregulation of ~44-fold ($P = 0.04$; Fig. 3C). The *Col4a1* level of SimpliDerm was increased to ~8-fold at 12 weeks, whereas that of AlloDerm RTU was significantly upregulated to ~154-fold ($P < 0.001$; Fig. 3D). These results reveal

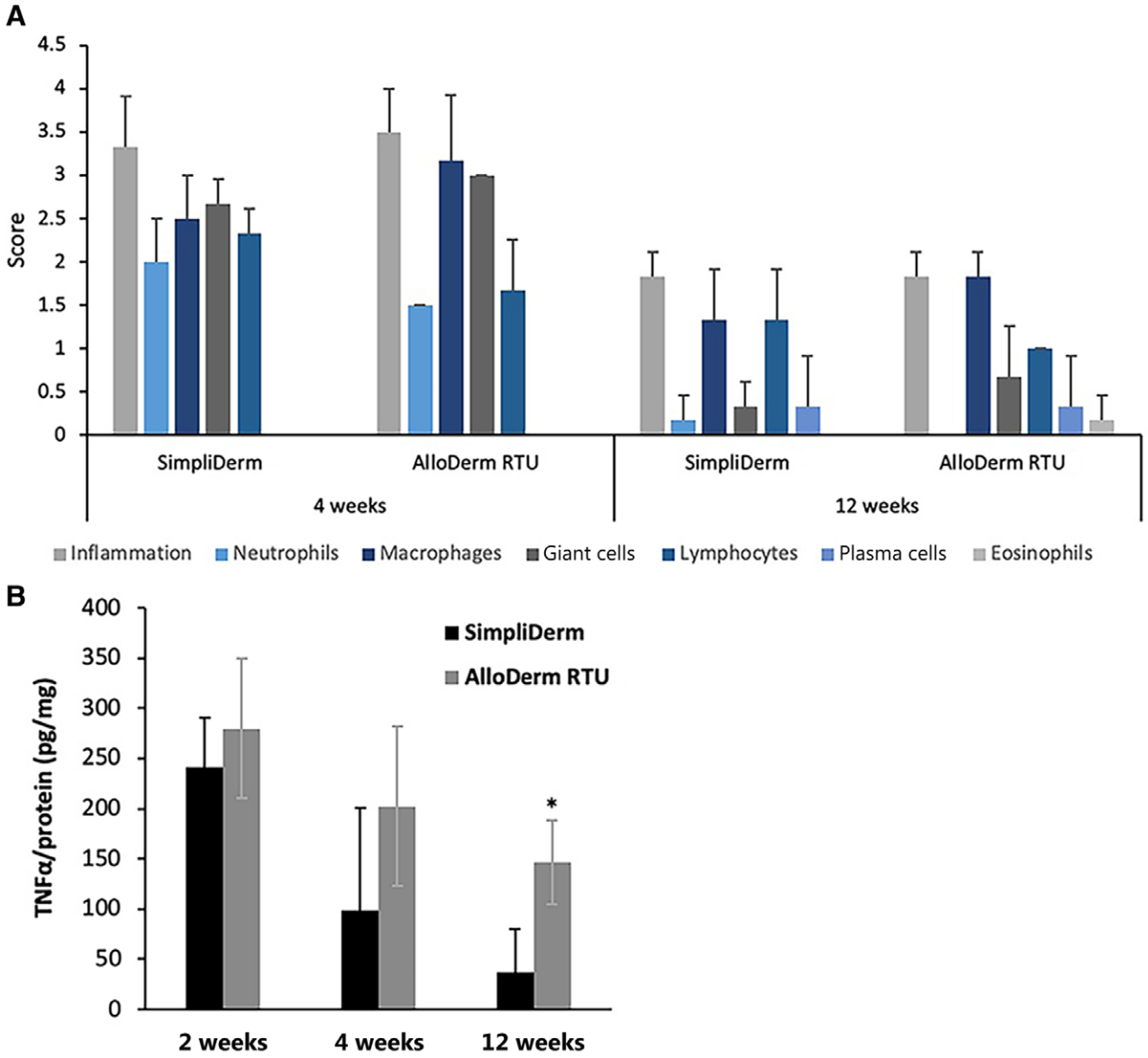

Fig. 2. Analysis of host inflammatory response in SimpliDerm and AlloDerm RTU implants. A, Histopathological evaluation score of general inflammation and inflammatory subtypes present in SimpliDerm and AlloDerm RTU implants at 4 weeks and 12 weeks. The score is based on the scoring matrix shown in Table 1. B, The amount of TNFα protein present in SimpliDerm and AlloDerm RTU implants for 2, 4, and 12-week time points as analyzed by ELISA. The error bar represents the calculated SD, with asterisk (*) representing $P < 0.05$ (actual $P = 0.034$).

that AlloDerm RTU implants showed a greater increase in the vascularization-associated gene expression than SimpliDerm implants over time.

Pro-fibrotic Responses

As chronic inflammatory responses to foreign materials can often lead to fibrosis, the levels of several fibrosis-associated genes[22–24] (*TGFβ1*, *CTGF*, *αSMA*, and *LH2b*) were investigated to assess pro-fibrotic responses in SimpliDerm and AlloDerm RTU implants over time. By 12 weeks, SimpliDerm exhibited significantly lower expression of all fibrosis-associated genes in comparison with AlloDerm RTU over time (Fig. 4). The *TGFβ1* expression level in SimpliDerm increased ~3-fold, whereas that in AlloDerm RTU increased ~4-fold ($P = 0.01$; Fig. 4A). The *αSMA* expression level for SimpliDerm showed a minimal fold-increase, whereas AlloDerm RTU showed ~6-fold-increase ($P = 0.006$; Fig. 4B). The *CTGF* expression level of SimpliDerm was ~4-fold higher and AlloDerm was ~13-fold higher ($P = 0.049$; Fig. 4C). The *LH2b* expression level for SimpliDerm was upregulated at ~8-fold although that for AlloDerm RTU was ~35-fold higher ($P = 0.027$; Fig. 4D). Collectively, the higher increase in the levels of fibrosis-related genes in AlloDerm RTU compared with SimpliDerm indicate a more pro-fibrotic environment in AlloDerm RTU over time.

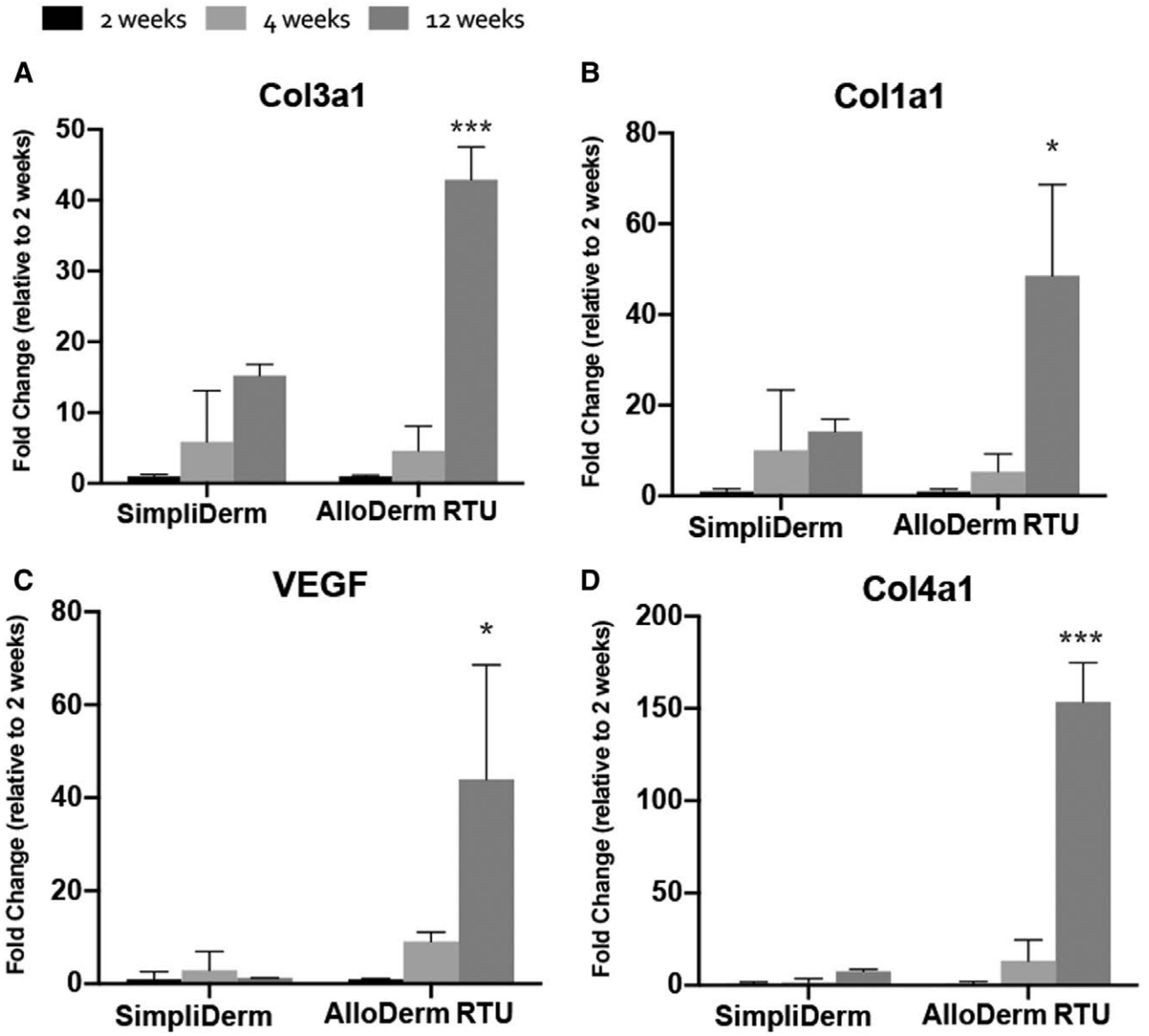

Fig. 3. Gene expression analysis related to collagen synthesis and vascularization. The relative gene expression levels (normalized to week 2 of each group) of key ECM components: *Col3a1* (A) and *Col1a1* (B), angiogenic factor *VEGF* (C), and blood vessel maturation marker *Col4a1* (D) in SimpliDerm and AlloDerm RTU implants for 2, 4, and 12-week time points. Error bars represent the calculated SD, with single asterisk (*) representing $P < 0.05$ (actual $P = 0.04$) (B, C) and triple asterisks (***) representing $P < 0.001$ (A, D).

DISCUSSION

A key consideration for evaluating hADM performance in surgical applications is that the hADM should provide a suitable scaffold to promote tissue remodeling while mitigating inflammation and fibrosis.[25] Thus, to explore these characteristics of 2 hADMs implants over time, an NHP model was utilized to characterize the temporal gene expression profiles and host tissue response. This animal was selected for their genomic similarity to the human genome, and therefore they are a valuable substitute for modeling the immunological response to hADM implants in humans.[12–14] Our histology and gene expression profiling results demonstrated a dynamic change in host tissue response from 2 to 12 weeks, and indicated a measurable difference between the hADM products tested, particularly in terms of the early inflammatory response and implant degradation rate.

At 4-weeks post-implantation, AlloDerm RTU showed a greater amount of inflammatory cells than SimpliDerm, as indicated by the CD68 immunostaining images. Further analysis into the cell subtypes showed that the macrophage population was higher than neutrophil population in AlloDerm RTU at 4 weeks ($P = 0.02$), whereas the 2 population amount was not significantly different in the SimpliDerm group. In the presence of an immune response stimulus, neutrophils are usually the first to respond and infiltrate the site of injury[26] and are subsequently engulfed by macrophages, which are of a pro-inflammatory (M1) phenotype at this early stage.[27]

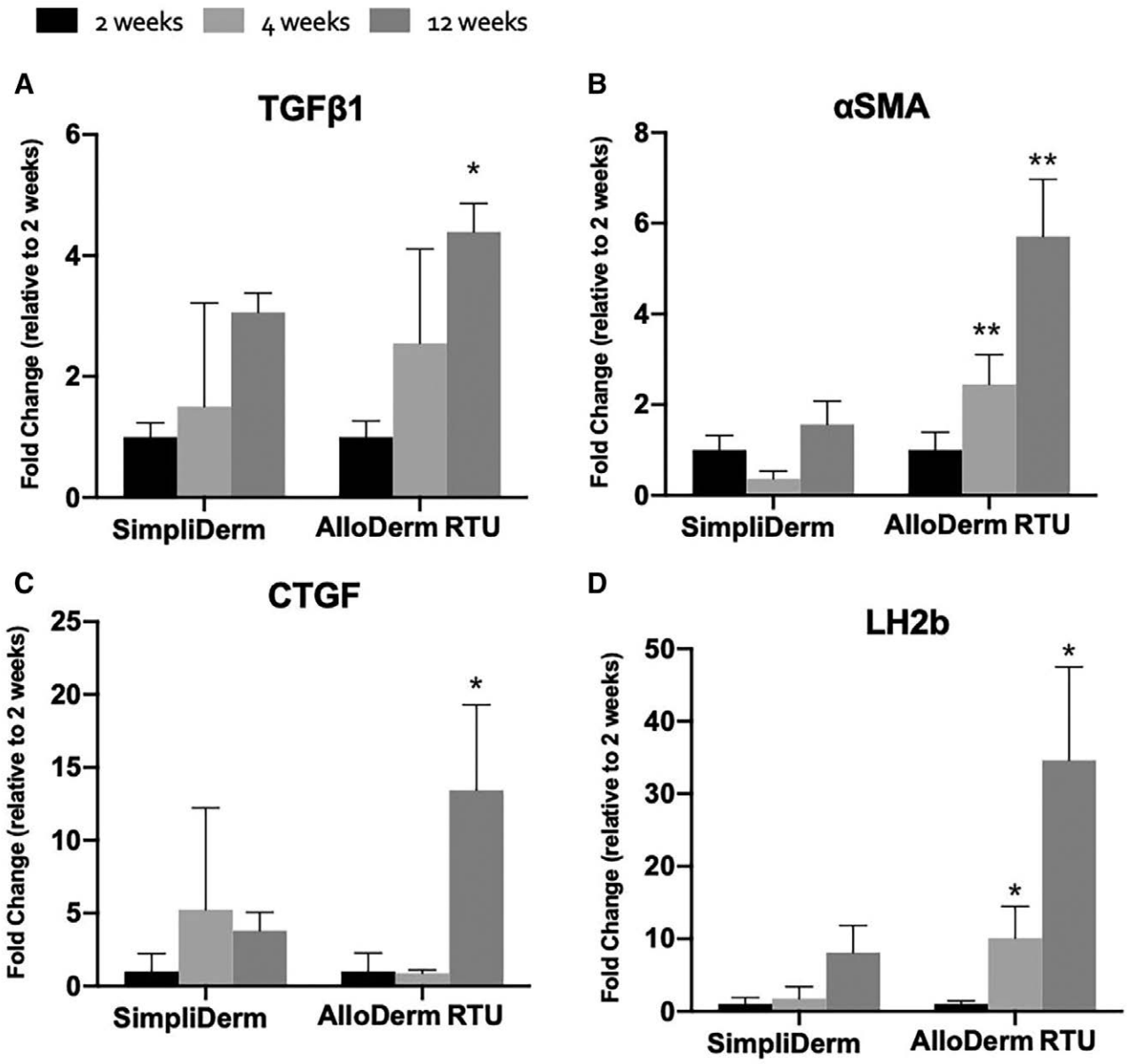

Fig. 4. Gene expression analysis related to fibrosis and matrix remodeling. The relative expression levels (normalized to week 2 of each group) of fibrosis-associated genes, including (A) *TGFβ1*, (B) *αSMA*, (C) *CTGF*, and (D) *LH2b* in SimpliDerm and AlloDerm RTU implants for 2, 4, and 12-week time points. Error bars represent the calculated SD, with single asterisk (*) representing $P < 0.05$ and double asterisks (**) representing $P < 0.01$. Actual P are (A) 0.01, (B) 0.006, (C) 0.049, and (D) 0.027.

Because macrophages of M1 phenotype engulf apoptotic neutrophils, the higher macrophage population that was present in AlloDerm RTU may have led to the decrease in its neutrophil population. This can also be implied that the early inflammatory response progressed slower in the SimpliDerm group. In fact, the pro-inflammatory environment persisted in AlloDerm RTU as measured by TNFα levels at 3 months, and was significantly higher than that in SimpliDerm.

The difference in the initial inflammatory response between SimpliDerm and AlloDerm RTU groups can be correlated with the implant degradation rate and ECM remodeling rate. H&E staining at 4 weeks indicated that implant degradation (loss in thickness) of AlloDerm RTU was much faster than SimpliDerm. Thus, the more rapid and higher inflammatory response shown in AlloDerm RTU TNFα levels can be correlated with faster degradation of the implant. Moreover, H&E staining from 4 weeks showed a more prominent cellular infiltration in AlloDerm RTU than SimpliDerm. Gene expression analysis of collagen synthesis and vascularization also indicated a significantly more rapid and greater remodeling rate in AlloDerm RTU than SimpliDerm. Although having no implant degradation at all is not desirable because it can impede cellular activity in situ,[28] expedited degradation, vascularization, and ECM

remodeling shown in AlloDerm RTU can also be viewed as unfavorable because it may correlate with increased fibrosis. Previous studies have indicated that events leading to fibrosis and scar formation are accompanied by increased secretion of pro-inflammatory cytokines and chemokines,[29] fibroblast proliferation, myofibroblast differentiation,[30] increased rate of vascularization through VEGF production,[31] and excessive collagen deposition.[32] A previous non-human primate study involving two commercially available hADM products demonstrated that the hADM with faster degradation resulted in capsule formation.[16] We observed similar results in this study: the expression levels of fibrosis-associated genes were significantly higher in AlloDerm RTU than in SimpliDerm at 12 weeks. Altogether our results showed that SimpliDerm achieved a more optimal hADM degradation profile than AlloDerm RTU, which is essential to promote healthy ECM remodeling and avoid fibrosis formation.

Because we used standardized implantation and analysis protocols for both hADMs, the different matrix properties of these implants must therefore be responsible for producing the distinct host inflammatory and fibrotic responses observed. Extensive efforts have been made to understand the effect of different tissue processing methods on hADM matrix integrity, and subsequently the host immune response.[11,33–35] The major differences in the manufacturing of both hADMs are most likely due to differing decellularization reagents, chemicals,[36,37] and terminal sterilization methods.[9,10] Because most of the processing reagents used are proprietary to each company, we are only able to comment on the sterilization methods of both implants. SimpliDerm is sterilized through gamma irradiation (to a Sterility Assurance Level (SAL) of 10^{-6}),[9] whereas AlloDerm RTU is sterilized through electron beam irradiation (to an SAL of 10^{-3}).[10] This difference alone may not explain the divergent in vivo results reported in this study, and unpublished in vitro data from our laboratory have shown that these processing methods do not result in a difference in matrix stability. Further studies are therefore warranted to evaluate the effect of other processing parameters on hADM performance.

Overall, histology and gene expression profiling analyses shown in this study demonstrate an effective model for analyzing hADM performance in terms of host inflammatory and fibrotic response. Our results indicated a lower initial inflammatory response and slower implant degradation rate in SimpliDerm implants. In addition, the gene expression levels of matrix remodeling factors and profibrotic markers indicated a more anti-inflammatory and pro-remodeling microenvironment within SimpliDerm. These results altogether indicate that SimpliDerm is able to promote productive tissue repair and regeneration within 3 months. Given the close immunological similarity between the African green monkey and humans, the current study may provide important insight into the potential human response to these hADM scaffolds. However, further studies are necessary to fully realize the clinical utility of this novel hADM.

Frank Fan, BS
Aziyo Biologics, Inc
12510 Prosperity Drive
Suite 370
Silver Spring, MD 20904
E-mail: ffan@aziyo.com

REFERENCES

1. Brewer MB, Rada EM, Milburn ML, et al. Human acellular dermal matrix for ventral hernia repair reduces morbidity in transplant patients. *Hernia*. 2011;15:141–145.
2. Garcia A, Baldoni A. Complex ventral hernia repair with a human acellular dermal matrix and component separation: a case series. *Ann Med Surg (Lond)*. 2015;4:271–278.
3. Venturi ML, Mesbahi AN, Boehmler JH IV, et al. Evaluating sterile human acellular dermal matrix in immediate expander-based breast reconstruction: a multicenter, prospective, cohort study. *Plast Reconstr Surg*. 2013;131:9e–18e.
4. Moyer HR, Hart AM, Yeager J, et al. A histological comparison of two human acellular dermal matrix products in prosthetic-based breast reconstruction. *Plast Reconstr Surg Glob Open*. 2017;5:e1576.
5. Banyard DA, Bourgeois JM, Widgerow AD, et al. Regenerative biomaterials: a review. *Plast Reconstr Surg*. 2015;135:1740–1748.
6. Sheikholeslam M, Wright MEE, Jeschke MG, et al. Biomaterials for Skin Substitutes. *Adv Healthc Mate*. 2018;7:1700897.
7. Brown BN, Badylak SF. Extracellular matrix as an inductive scaffold for functional tissue reconstruction. *Transl Res*. 2014;163:268–285.
8. Dziki JL, Huleihel L, Scarritt ME, et al. Extracellular matrix bioscaffolds as immunomodulatory biomaterials. *Tissue Eng Part A*. 2017;23:1152–1159.
9. AziyoBiologics. Simpliderm hydrated acellular dermal matrix: instructions for use. *Aziyo Biol*. 2019;1–2.
10. Allergan. *AlloDerm Select Regenerative Tissue Matrix: Instructions for Use*. Branchburg, N.J.: Allergan; 2020.
11. Sun WQ, Xu H, Sandor M, et al. Process-induced extracellular matrix alterations affect the mechanisms of soft tissue repair and regeneration. *J Tissue Eng*. 2013;4:2041731413505305.
12. Warren WC, Jasinska AJ, García-Pérez R, et al. The genome of the vervet (*Chlorocebus aethiops sabaeus*). *Genome Res*. 2015;25:1921–1933.
13. Stump A, Holton LH III, Connor J, et al. The use of acellular dermal matrix to prevent capsule formation around implants in a primate model. *Plast Reconstr Surg*. 2009;124:82–91.
14. Xu H, Wan H, Sandor M, et al. Host response to human acellular dermal matrix transplantation in a primate model of abdominal wall repair. *Tissue Eng Part A*. 2008;14:2009–2019.
15. Hérodin F, Thullier P, Garin D, et al. Nonhuman primates are relevant models for research in hematology, immunology and virology. *Eur Cytokine Netw*. 2005;16:104–116.
16. Sandor M, Singh D, Silverman RP, et al. Comparative host response of 2 human acellular dermal matrices in a primate implant model. *Eplasty*. 2014;14:e7.
17. Sandor M, Leamy P, Assan P, et al. Relevant *In Vitro* predictors of human acellular dermal matrix-associated inflammation and capsule formation in a nonhuman primate subcutaneous tissue expander model. *Eplasty*. 2017;17:e1.
18. Le SJ, Gongora M, Zhang B, et al. Gene expression profile of the fibrotic response in the peritoneal cavity. *Differentiation*. 2010;79:232–243.
19. Luttikhuizen DT, Dankers PY, Harmsen MC, et al. Material dependent differences in inflammatory gene expression by giant cells during the foreign body reaction. *J Biomed Mater Res A*. 2007;83:879–886.

20. Ye J, Coulouris G, Zaretskaya I, et al. Primer-BLAST: a tool to design target-specific primers for polymerase chain reaction. *BMC Bioinformatics*. 2012;13:134.
21. Haimes J, Kelley M. Demonstration of a ΔΔCq calculation method to compute relative gene expression from qPCR data. *Thermo Scientific Tech Note*. 2010;104.
22. Ihn H. Pathogenesis of fibrosis: role of TGF-beta and CTGF. *Curr Opin Rheumatol*. 2002;14:681–685.
23. Rao K B, Malathi N, Narashiman S, et al. Evaluation of myofibroblasts by expression of alpha smooth muscle actin: a marker in fibrosis, dysplasia and carcinoma. *J Clin Diagn Res*. 2014;8:ZC14–ZC17.
24. van der Slot AJ, Zuurmond AM, van den Bogaerdt AJ, et al. Increased formation of pyridinoline cross-links due to higher telopeptide lysyl hydroxylase levels is a general fibrotic phenomenon. *Matrix Biol*. 2004;23:251–257.
25. Londono R, Badylak SF. Biologic scaffolds for regenerative medicine: mechanisms of *in vivo* remodeling. *Ann Biomed Eng*. 2015;43:577–592.
26. Kim MH, Liu W, Borjesson DL, et al. Dynamics of neutrophil infiltration during cutaneous wound healing and infection using fluorescence imaging. *J Invest Dermatol*. 2008;128:1812–1820.
27. Das A, Sinha M, Datta S, et al. Monocyte and macrophage plasticity in tissue repair and regeneration. *Am J Pathol*. 2015;185:2596–2606.
28. Carletti E, Motta A, Migliaresi C. Scaffolds for tissue engineering and 3D cell culture. *Methods Mol Biol*. 2011;695:17–39.
29. Novak ML, Koh TJ. Macrophage phenotypes during tissue repair. *J Leukoc Biol*. 2013;93:875–881.
30. Wang YY, Jiang H, Pan J, et al. Macrophage-to-myofibroblast transition contributes to interstitial fibrosis in chronic renal allograft injury. *J Am Soc Nephrol*. 2017;28:2053–2067.
31. Wilgus TA, Ferreira AM, Oberyszyn TM, et al. Regulation of scar formation by vascular endothelial growth factor. *Lab Invest*. 2008;88:579–590.
32. Coelho NM, McCulloch CA. Contribution of collagen adhesion receptors to tissue fibrosis. *Cell Tissue Res*. 2016;365:521–538.
33. Keane TJ, Londono R, Turner NJ, et al. Consequences of ineffective decellularization of biologic scaffolds on the host response. *Biomaterials*. 2012;33:1771–1781.
34. Faulk DM, Carruthers CA, Warner HJ, et al. The effect of detergents on the basement membrane complex of a biologic scaffold material. *Acta Biomater*. 2014;10:183–193.
35. Londono R, Dziki JL, Haljasmaa E, et al. The effect of cell debris within biologic scaffolds upon the macrophage response. *J Biomed Mater Res A*. 2017;105:2109–2118.
36. Taufique ZM, Bhatt N, Zagzag D, et al. Revascularization of alloderm used during endoscopic skull base surgery. *J Neurol Surg B Skull Base*. 2019;80:46–50.
37. Hinchcliff KM, Orbay H, Busse BK, et al. Comparison of two cadaveric acellular dermal matrices for immediate breast reconstruction: a prospective randomized trial. *J Plast Reconstr Aesthet Surg*. 2017;70:568–576.